HERA Inclusive Diffraction & Factorisation Tests

Paul Newman (for the H1 and ZEUS Collaborations)

School of Physics & Astronomy, University of Birmingham, B15 2TT, UK

HERA measurements of diffractive ep scattering - the quasi-elastic scattering of the photon in the proton colour field - are summarised. Emphasis is placed on the most recent data.

1   Introduction

Between 1992 and 2007, the HERA accelerator provided ep collisions at centre of mass energies beyond 300 GeV at the interaction points of the H1 and ZEUS experiments. Perhaps the most interesting results to emerge relate to the newly accessed field of perturbative strong interaction physics at low Bjorken-x, where parton densities become extremely large [1]. Questions arise as to how and where non-linear dynamics tame the parton density growth [2] and challenging features such as geometric scaling [3] are observed. Central to this low x physics landscape is a high rate of diffractive processes, in which a colourless exchange takes place and the proton remains intact. In particular, the study of semi-inclusive diffractive deep-inelastic scattering (DDIS), $\gamma^* p \to Xp$ [4] has led to a revolution in our microscopic, parton level, understanding of the structure of elastic and quasi-elastic high energy hadronic scattering [5]. Comparisons with hard diffraction in proton-(anti)proton scattering have also improved our knowledge of absorptive and underlying event effects in which the diffractive signature may be obscured by multiple interactions in the same event [6]. In addition to their fundamental interest in their own right, these issues are highly relevant to the modelling of chromodynamics at the LHC [7].

The kinematic variables describing DDIS are illustrated in figure 1a. The longitudinal momentum fractions of the colourless exchange with respect to the incoming proton and of the struck quark with respect to the colourless exchange are denoted $x_{I\!P}$ and β, respectively, such that $\beta x_{I\!P} = x$. The squared four-momentum transferred at the proton vertex is given by the Mandelstam t variable. The semi-inclusive DDIS cross section is usually presented in the form of a diffractive reduced cross section $\sigma_r^{D(3)}$, integrated over t and related to the experimentally measured differential cross section by [8]

$$\frac{\mathrm{d}^3 \sigma^{ep \to eXp}}{\mathrm{d}x_{I\!P} \; \mathrm{d}x \; \mathrm{d}Q^2} = \frac{2\pi\alpha^2}{xQ^4} \cdot Y_+ \cdot \sigma_r^{D(3)}(x_{I\!P}, x, Q^2) \;, \tag{1}$$

where $Y_+ = 1 + (1-y)^2$ and y is the usual Bjorken variable. The reduced cross section depends at moderate scales, Q^2, on two diffractive structure functions $F_2^{D(3)}$ and $F_L^{D(3)}$ according to

$$\sigma_r^{D(3)} = F_2^{D(3)} - \frac{y^2}{Y_+} F_L^{D(3)}. \tag{2}$$

For y not too close to unity, $\sigma_r^{D(3)} = F_2^{D(3)}$ holds to very good approximation.
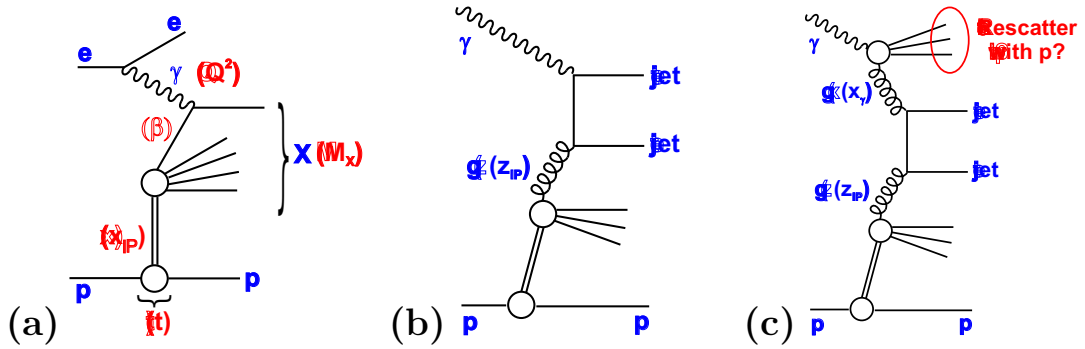
Figure 1: Sketches of diffractive ep processes. (a) Inclusive DDIS at the level of the quark parton model, illustrating the kinematic variables discussed in the text. (b) Dominant leading order diagram for hard scattering in DDIS or direct photoproduction, in which a parton of momentum fraction $z_{I\!P}$ from the DPDFs enters the hard scattering. (c) A leading order process in resolved photoproduction involving a parton of momentum fraction x_γ relative to the photon.

2 Measurement methods and comparisons

Experimentally, diffractive ep scattering is characterised by the presence of a leading proton in the final state, retaining most of the initial state proton energy, and by a lack of hadronic activity in the forward (outgoing proton) direction, such that the system X is cleanly separated and its mass M_X may be measured in the central detector components. These signatures have been widely exploited at HERA to select diffractive events by tagging the outgoing proton in the H1 Forward Proton Spectrometer or the ZEUS Leading Proton Spectrometer ('LPS method' [9, 10, 11]) or by requiring the presence of a large gap in the rapidity distribution of hadronic final state particles in the forward region ('LRG method' [8, 10, 12]). In a third approach, not considered in detail here, the inclusive DIS sample is decomposed into diffractive and non-diffractive contributions based on their characteristic dependences on M_X [12, 13]. Whilst the LRG and M_X-based techniques yield better statistics than the LPS method, they suffer from systematic uncertainties associated with an admixture of proton dissociation to low mass states, which is irreducible due to the limited forward detector acceptance.

The H1 collaboration recently released a preliminary proton-tagged measurement using its full available FPS sample at HERA-II [11]. The integrated luminosity is 156 pb^{-1}, a factor of 20 beyond previous H1 measurements. The new data tend to lie slightly above the recently published final ZEUS LPS data from HERA-I [10], but are within the combined normalisation uncertainty of around 10%. The most precise test of compatibility between H1 and ZEUS is obtained from the LRG data. The recently published ZEUS data [10] are based on an integrated luminosity of 62 pb^{-1} and thus have substantially improved statistical precision compared with the older H1 published results [8]. The normalisation differences between the two experiments are most obvious here, having been quantified at 13%, which is a little beyond one standard deviation in the combined normalisation uncertainty. After correcting for this factor, very good agreement is observed between the shapes of the H1 and ZEUS cross sections throughout most of the phase space studied, as shown in figure 2. A more detailed comparison between different diffractive cross section measurements by H1 and ZEUS and a first attempt to combine the results of the two experiments can be found in [14].
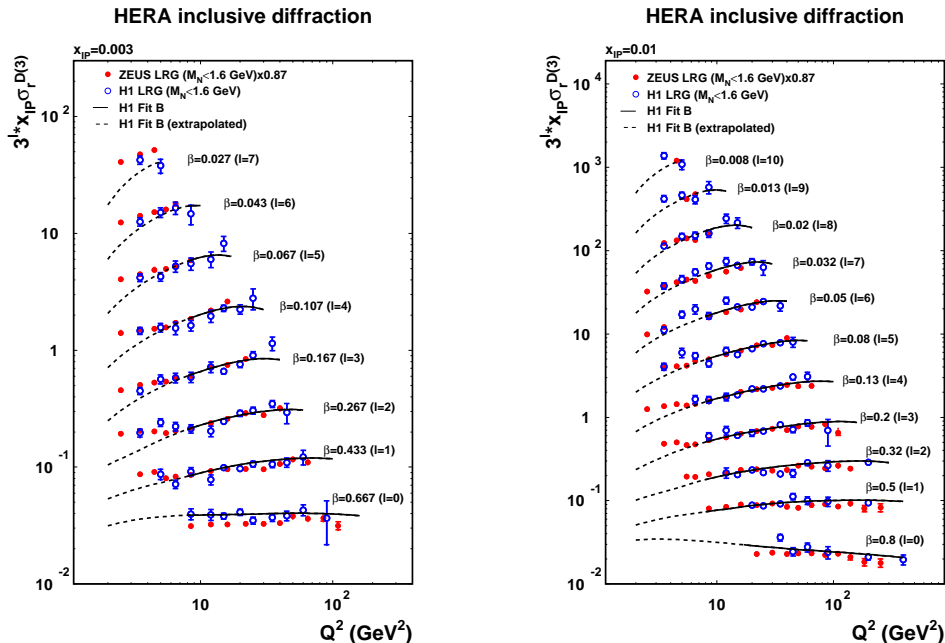
Figure 2: H1 and ZEUS measurements of the diffractive reduced cross section at two example $x_{I\!P}$ values [14]. The ZEUS data are scaled by a factor of 0.87 to match the H1 normalisation. The data are compared with the results of the H1 2006 Fit B DPDF based parameterisation [8] for $Q^2 \geq 8.5$ GeV^2 and with its DGLAP based extrapolation to lower Q^2.

3   Soft physics at the proton vertex

To good approximation, LRG and LPS data show [8, 9, 10] that DDIS data satisfy a 'proton vertex factorisation',[1] whereby the dependences on variables which describe the scattered proton $(x_{I\!P}, t)$ factorise from those describing the hard partonic interaction (Q^2, β). For example, the slope parameter b, extracted in [10] by fitting the t distribution to the form $\mathrm{d}\sigma/\mathrm{d}t \propto e^{bt}$, is shown as a function of DDIS kinematic variables in figure 3a. There are no significant variations from the average value of $b \simeq 7$ GeV^{-2} anywhere in the studied range. The measured value of b is significantly larger than that from 'hard' exclusive vector meson production $(ep \to eVp)$ [15]. It is characteristic of an interaction region of spatial extent considerably larger than the proton radius, indicating that the dominant feature of DDIS is the probing with the virtual photon of non-perturbative exchanges similar to the pomeron of soft hadronic physics [18].

Figure 3b shows the Q^2 dependence of the effective pomeron intercept $\alpha_{I\!P}(0)$, which is extracted from the $x_{I\!P}$ dependence of the data [10]. No significant dependence on Q^2 is observed, again compatible with proton vertex factorisation. These results are consistent with the H1

---

[1]This factorisation is not expected to hold to indefinite precision, due for example to the presence of a 'hard', fully perturbatively tractable diffractive exchange which governs exclusive vector meson production in the presence of hard scales [15]. This leads to a higher twist contribution to σ_r^D for $\beta \to 1$ [16, 17]. However, this contribution seems to be numerically small when compared with the the inclusive diffractive cross section.
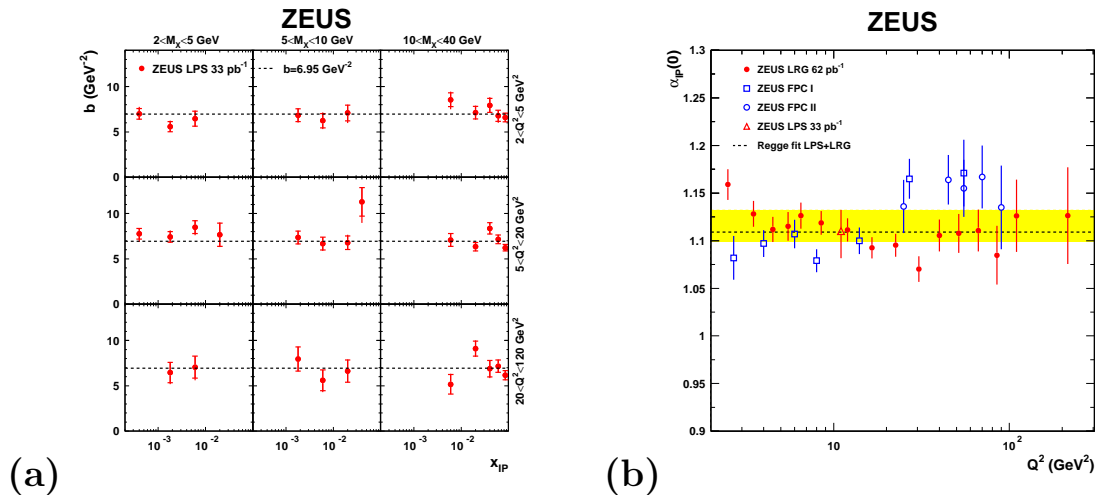
Figure 3: a) Measurements of the exponential t slope from ZEUS LPS data, shown as a function of Q^2, $x_{I\!P}$ and M_X. b) ZEUS extractions of the effective pomeron intercept describing the $x_{I\!P}$ dependence of DDIS data at different Q^2 values [10].

value of $\alpha_{I\!P}(0) = 1.118 \pm 0.008$ (exp.) $^{+0.029}_{-0.010}$ (model) [8]. Both collaborations have also extracted a value for the slope of the effective pomeron trajectory, the recently published ZEUS value being $\alpha'_{I\!P} = -0.01 \pm 0.06$ (stat.) ± 0.06 (syst.) GeV^{-2} [10].

The intercept of the effective pomeron trajectory is consistent within errors with the 'soft pomeron' results from fits to total cross sections and soft diffractive data [19]. Although larger effective intercepts have been measured in hard vector meson production [15], no deviations with either Q^2 or β have yet been observed in inclusive DDIS. The measured slope of the effective trajectory is smaller than the canonical soft diffractive value of 0.25 GeV^{-2} [20], though it is compatible with results from the soft exclusive photoproduction of ρ^0 mesons at HERA [21].

4 Diffractive Parton Density Functions

In the framework of the proof [22] of a hard scattering collinear QCD factorisation theorem for semi-inclusive DIS processes such as DDIS, the concept of 'diffractive parton distribution functions' (DPDFs) [23] may be introduced, representing conditional proton parton probability distributions under the constraint of a leading final state proton with a particular four-momentum. The differential DDIS cross section may then be written in terms of convolutions of partonic cross sections $\hat{\sigma}^{ei}(x, Q^2)$ with DPDFs f_i^D as

$$\mathrm{d}\sigma^{ep \to eXp}(x, Q^2, x_{I\!P}, t) = \sum_i f_i^D(x, Q^2, x_{I\!P}, t) \otimes \mathrm{d}\hat{\sigma}^{ei}(x, Q^2) . \tag{3}$$

The empirically motivated proton vertex factorisation property (section 3) suggests a further factorisation, whereby the DPDFs vary only in normalisation with the four-momentum of the final state proton as described by $x_{I\!P}$ and t:

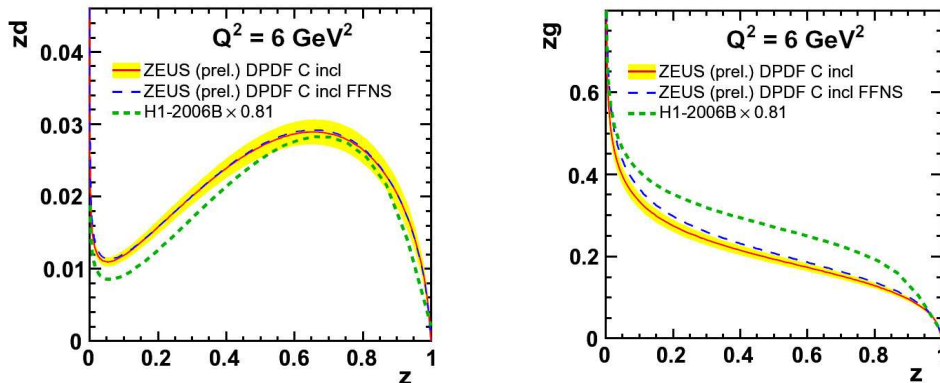$$f_i^D(x, Q^2, x_{I\!P}, t) = f_{I\!P/p}(x_{I\!P}, t) \cdot f_i(\beta = x/x_{I\!P}, Q^2) . \tag{4}$$

Figure 4: ZEUS down quark (one sixth of the total quark + antiquark) and gluon densities as a function of generalised momentum fraction z at $Q^2 = 6$ GeV^2 [25]. Two heavy flavour schemes are shown, as well as H1 results [8] corrected for proton dissociation with a factor of 0.81.

Parameterising $f_{I\!P/p}(x_{I\!P}, t)$ using Regge asymptotics, equation 4 amounts to a description of DDIS in terms of the exchange of a factorisable pomeron with universal parton densities [24]. The β and Q^2 dependences of σ_r^D may then be subjected to a perturbative QCD analysis based on the DGLAP equations in order to obtain DPDFs. Whilst F_2^D directly measures the quark density, the gluon density is only indirectly constrained, via the scaling violations $\partial F_2^D / \partial \ln Q^2$.

The high statistics ZEUS LRG and LPS data [10] have recently been fitted to extract DPDFs [25]. The method and DPDF parameterisation are similar to an earlier H1 analysis [8], the main step forward being in the heavy flavour treatment, which now follows the general mass variable flavour number scheme [26]. In figure 4, the resulting DPDFs are compared with results from both ZEUS and H1 using a fixed flavour number scheme. The agreement between the experiments is reasonable when the uncertainty on the H1 DPDFs is also taken into account and the conclusion that the dominant feature is a gluon density with a relatively hard z dependence is confirmed. The error bands shown in figure 4 represent experimental uncertainties only. Whilst the quark densities are rather well known throughout the phase space, the theoretical uncertainties on the gluon density are large. Indeed, in the large z region, where the dominant parton splitting is $q \rightarrow qg$, the sensitivity of $\partial F_2^D / \partial \ln Q^2$ to the gluon density becomes poor and different DPDF parameterisations lead to large variations [8, 25]. Improved large z constraints have been obtained by including dijet data in the QCD fits [27, 25].

In common with the inclusive proton PDFs at low x [1], the DPDFs exhibit a ratio of around 7:3 between gluons and quarks, consistent with a common QCD radiation pattern far from the valence region. Qualitatively, the diffractive quark density is similar in shape to that of the photon [28], which might be expected if the high z quarks are generated from initial basic $g \rightarrow q\bar{q}$ splittings, similar to the $\gamma \rightarrow q\bar{q}$ splitting in the photon case.

5   Factorisation Tests in Diffractive DIS

According to [22], the diffractive parton densities extracted from σ_r^D should be applicable to the prediction of a wide range of other observables in diffractive DIS. There have been many tests of
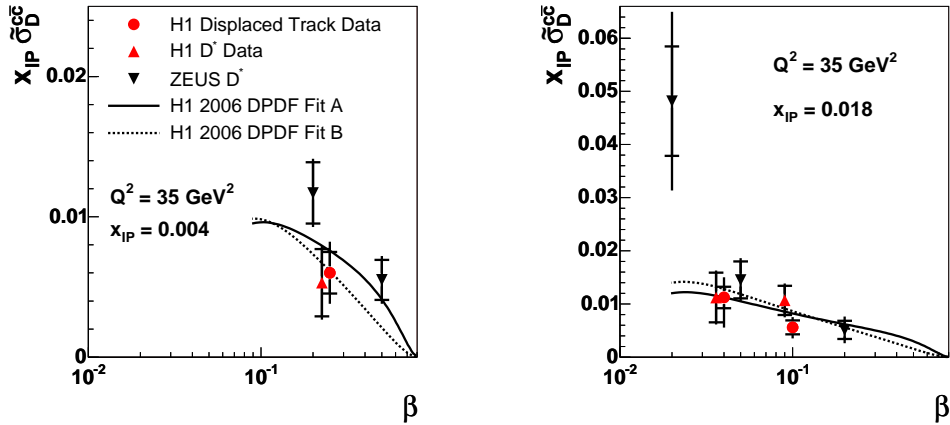
Figure 5: Comparisons [32] of measurements of diffractive open charm production with predictions based on DPDFs extracted from σ_r^D data [8].

this diffractive hard scattering factorisation over the years, the most precise and detailed arising from jet [29, 30, 27] and heavy flavour [31, 32] cross section measurements. Being dominated by the boson-gluon fusion parton level process $\gamma^* g \to q\bar{q}$ (figure 1b), these data are directly sensitive to the diffractive gluon density, in contrast to σ_r^D. Such tests have been successful at moderate values of z, as shown for the example of diffractive charm quark production in figure 5. As mentioned in section 4, the situation changes at large $z \gtrsim 0.4$, where the gluon density from σ_r^D has a large uncertainty and dijet data give the best constraints.

At low x and Q^2, the longitudinal diffractive structure function, F_L^D, is closely related to the diffractive gluon density [33] and thus gives a complementary test of diffractive factorisation and the role of gluons to those provided by jet and charm cross sections. Measurements of F_L^D became possible following the reduced proton beam energy runs at the end of HERA operation. According to equation 2, F_L^D and F_2^D may then be separated through the $y = Q^2/(s\,\beta\,x_{I\!P})$ dependence as s varies at fixed Q^2, β and $x_{I\!P}$.

The H1 collaboration recently released preliminary F_L^D data, as shown in figure 6. The results [34], when integrated over β show that F_L^D is non-zero at the 3σ level. It is also clearly incompatible with its maximum possible value of F_2^D. The measured ratio of longitudinal to transverse photon induced cross sections in diffraction is similar to that in inclusive DIS measurements [35], though the errors in the

Figure 6: First measurement of the longitudinal diffractive structure function [34], compared with DPDF based predictions.

diffractive case are large. The measured F_L^D is in agreement with all reasonable predictions based on DPDFs extracted from σ_r^D. Dipole model predictions such as [2, 16] have thus far
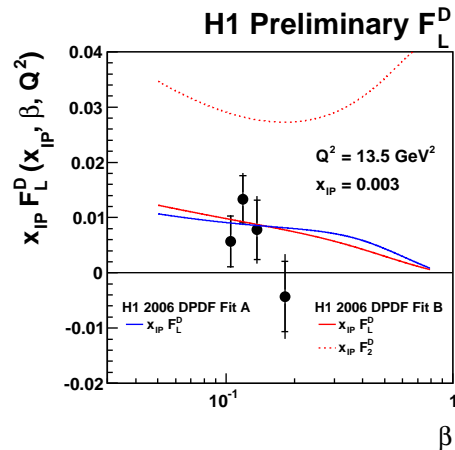
neglected any contribution from a leading twist F_L^D and formally give predictions very close to zero in the relatively low β range covered. A hybrid approach [36] which mixes a leading twist DPDF based F_L^D with a higher twist contribution at high β derived from [2], is in good agreement with the data.

6 Hard Diffractive Photoproduction and Rapidity Gap Survival Probabilities

As expected [22, 37], DPDF-based predictions for hard diffractive processes in $p\bar{p}$ scattering fail by around an order of magnitude [38]. This factorisation breaking is generally attributed to absorptive corrections, corresponding to the destruction of the outgoing proton coherence and the rapidity gap due to multiple interactions within a single event. These effects are associated with the presence of a proton remnant, in contrast to the point-like photon coupling in DDIS. The corresponding 'rapidity gap survival probability' can be treated semi-quantitatively [6] and its prediction at LHC energies is a major current issue [7].

The questions of DPDF applicability and rapidity gap survival can be addressed in hard diffractive photoproduction, where the virtuality of the exchange photon coupling to the electron is close to zero [39]. Under these circumstances, the photon can develop an effective partonic structure via $\gamma \to q\bar{q}$ fluctuations and further subsequent splittings. In a simple leading order picture, there are thus two classes of hard photoproduction: 'resolved' interactions (figure 1c), where the photon interacts via its partonic structure and only a fraction x_γ of its four-momentum participates in the hard subprocess and 'direct' interactions (figure 1b), where the photon behaves as a point-like particle and $x_\gamma = 1$. The gap survival probability has been estimated to be 0.34 for resolved processes [40] and is expected to be unity for direct photon interactions.

Figure 7 [41] shows ratios of H1 measurements of diffractive dijet photoproduction cross sections to NLO QCD calculations which neglect absorptive effects [42]. Results are shown differentially in the leading jet transverse energy E_T^{jet1} and in

Figure 7: Ratios of diffractive dijet photoproduction cross sections measured by H1 to NLO QCD calculations [41].

hadron level estimators of $z_{I\!P}$ and x_γ, obtained as described in [30]. For most of the measured points, the ratios are significantly below unity. When taking the H1 Fit B DPDFs [8], which
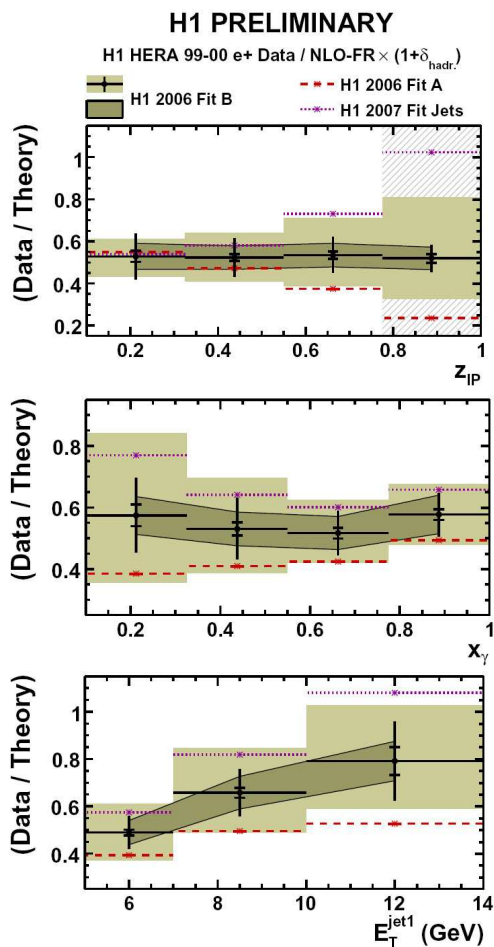
describe a wide range of DDIS observables, there is little dependence of the ratio on $z_{I\!P}$.

Figure 8 shows a recent ZEUS measurement [43] as a function of x_γ compared with predictions based on H1 [27] and ZEUS [25] DPDFs extracted by fitting σ_r^D and diffractive dijet electroproduction data. In contrast to the H1 case, these data are compatible with NLO predictions. A possible explanation for the apparent discrepancy between the two collaborations is offered by indications of a dependence of the data-to-theory ratio on the jet transverse energy (figure 7c) [30, 43, 41]. The ZEUS measurement is made for $E_t^{\text{jet1}} > 7.5$ GeV, whereas H1 measure for $E_t^{\text{jet1}} > 5$ GeV. There is as yet no accepted theoretical explanation for this effect.

Intriguingly, the ratios of data to theory measured by both collaborations have at most a weak dependence on x_γ, in contrast to theoretical expectations [40, 44]. Since the correlations between the variables are complicated (e.g. E_T^{jet1} and x_γ are strongly positively correlated through the kinematic restrictions), more differential studies are required to fully unfold the dynamics.
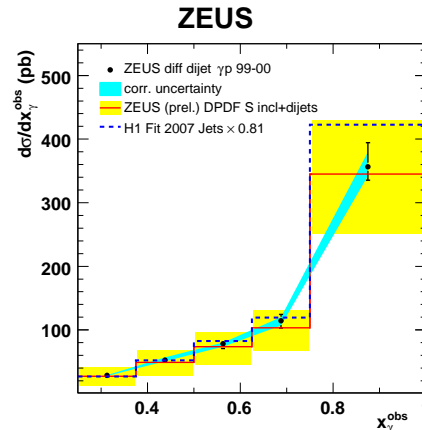

Figure 8: ZEUS diffractive dijet photoproduction data [43], compared with DPDF based predictions.

7 Summary

Recent H1 and ZEUS semi-inclusive diffractive DIS (DDIS) data are in fair agreement within their normalisation uncertainties. The data exhibit proton vertex factorisation to good approximation. Dependences on variables describing the coupling to the proton lead to a picture in which DDIS probes a diffractive exchange whose origins lie in the soft dynamics below typical factorisation scales, and which is similar to that exchanged in soft hadronic scattering. The parton densities (DPDFs) associated with this exchange have a structure dominated by a hard gluon density, which successfully describes all measured observables in diffractive DIS, including the longitudinal diffractive structure function, F_L^D. The rapidity gap survival probability derived from DPDF-based predictions of hard diffractive photoproduction data is surprisingly similar for direct and resolved photon interactions, a fact which remains under investigation.

References

[1] M. Klein, these proceedings.

[2] K. Golec-Biernat, M. Wüsthoff, Phys. Rev. D **59** (1999) 014017 [hep-ph/9807513].

[3] A. Stasto, K. Golec-Biernat, J. Kwiecinski, Phys. Rev. Lett. **86** (2001) 596 [hep-ph/0007192].

[4] ZEUS Collaboration, Phys. Lett. B **315** (1993) 481;
H1 Collaboration, Nucl. Phys. B **429** (1994) 477.

[5] A. Hebecker, Phys. Rept. **331** (2000) 1 [hep-ph/9905226].

[6] A. Kaidalov, V. Khoze, A. Martin, M. Ryskin, Eur. Phys. J. C **21** (2001) 521 [hep-ph/0105145].

[7] M. Arneodo, M. Diehl, V. Khoze, P. Newman, proc. of the 2006-8 HERA-LHC Workshop, DESY-PROC-2009-02, 397, and references therein.

[8] H1 Collaboration, Eur. Phys. J. C **48** (2006) 715 [hep-ex/0606004].

[9] H1 Collaboration, Eur. Phys. J. C **48** (2006) 749 [hep-ex/0606003].

[10] ZEUS Collaboration, Nucl. Phys. B **816** (2009) 1 [hep-ex/0812.2003].

[11] H1 Collaboration, *'Measurement of diffractive DIS with a leading proton at HERA-2'* [H1prelim-09-012].

[12] H1 Collaboration, *'Measurement of Inclusive Diffractive DIS at HERA (99-04 data)'* [H1prelim-06-014].

[13] ZEUS Collaboration, Nucl. Phys. B **800** (2008) 1 [hep-ex/0802.3017].

[14] P. Newman, M. Ruspa, proc. of the 2006-8 HERA-LHC Workshop, DESY-PROC-2009-02, 401 [hep-ex/0903.2957].

[15] S. Kananov, these proceedings.

[16] J. Bartels, J. Ellis, H. Kowalski, M. Wüsthoff, Eur. Phys. J. C **7** (1999) 443 [hep-ph/9803497].

[17] A. Hebecker, T. Teubner, Phys. Lett. B **498** (2001) 16 [hep-ph/0010273].

[18] E. Feinberg, I. Pomeranchuk, Suppl. Nuovo. Cimento. **3** (1956) 652;
V. Gribov, JETP Lett. **41** (1961) 667.

[19] A. Donnachie, P. Landshoff, Phys. Lett. B **296** (1992) 227 [hep-ph/9209205];
J. Cudell, K. Kang, S. Kim, Phys. Lett. B **395** (1997) 311 [hep-ph/9601336].

[20] G. Jaroszkiewicz, P. Landshoff, Phys. Rev. D **10** (1974) 170;
P. Landshoff, Nucl. Phys. Proc. Suppl. **12** (1990) 397.

[21] ZEUS Collaboration, Eur. Phys. J. C **14** (2000) 213 [hep-ex/9910038];
H1 Collaboration, *'Measurement of Pomeron Trajectory in Elastic ρ^0 Photoproduction'* [H1prelim-06-016]

[22] J. Collins, Phys. Rev. D **57** (1998) 3051 [Erratum-ibid. D **61** (2000) 019902] [hep-ph/9709499].

[23] L. Trentadue, G. Veneziano, Phys. Lett. B **323** (1994) 201;
A. Berera, D. Soper, Phys. Rev. D **53** (1996) 6162 [hep-ph/9509239].

[24] G. Ingelman, P. Schlein, Phys. Lett. B **152** (1985) 256;
A. Donnachie, P. Landshoff, Phys. Lett. B **191** (1987) 309 [Erratum-ibid. B **198** (1987) 590].

[25] ZEUS Collaboration, *'A QCD analysis of diffractive DIS data from ZEUS'* [ZEUS-pub-09-010].

[26] R. Thorne, R. Roberts, Phys. Rev. D **57** (1998) 6871 [hep-ph/9709442].

[27] H1 Collaboration, JHEP **0710** (2007) 042 [hep-ex/0708.3217].

[28] R. Nisius, these proceedings.

[29] H1 Collaboration, Eur. Phys. J. C **20** (2001) 29 [hep-ex/0012051];
ZEUS Collaboration, Eur. Phys. J. C **52** (2007) 813 [hep-ex/0708.1415].

[30] H1 Collaboration, Eur. Phys. J. C **51** (2007) 549 [hep-ex/0703022].

[31] H1 Collaboration, Phys. Lett. B **520** (2001) 191 [hep-ex/0108047];
ZEUS Collaboration, Nucl. Phys. B **672** (2003) 3 [hep-ex/0307068].

[32] H1 Collaboration, Eur. Phys. J. C **50** (2007) 1 [hep-ex/0610076].

[33] P. Newman, proc. of the 2004-5 HERA-LHC Workshop, CERN-2005-014, 514 [hep-ex/0511047].

[34] H1 Collaboration, *'Measurement of F_L^D at HERA II'* [H1prelim-09-011].

[35] H1 Collaboration, Phys. Lett. B **665** (2008) 139 [hep-ex/0805.2809];
ZEUS Collaboration, DESY 09-046 [hep-ex/0904.1092].

[36] K. Golec-Biernat, A. Luszczak, Phys. Rev. D **76** (2007) 114014 [hep-ph/0704.1608].

[37] J. Collins, L. Frankfurt, M. Strikman, Phys. Lett. B **307** (1993) 161 [hep-ph/9212212];
A. Berera, D. Soper, Phys. Rev. D **50** (1994) 4328 [hep-ph/9403276].

[38] CDF Collaboration, Phys. Rev. Lett. **84** (2000) 5043;
M. Klasen, G. Kramer, [hep-ph/0908.2531].

[39] J. Butterworth, M. Wing, Rept. Prog. Phys. **68** (2005) 2773 [hep-ex/0509018].

[40] A. Kaidalov, V. Khoze, A. Martin, M. Ryskin, Phys. Lett. B **567** (2003) 61 [hep-ph/0306134].

[41] H1 Collaboration, *'Diffractive photoproduction of jets with the H1 detector '* [H1prelim-08-012].

[42] S. Frixione, Z. Kunzst, A. Signer, Nucl. Phys. B **467** (1996) 399 [hep-ph/9512328];
S. Frixione, Nucl. Phys. B **507** (1997) 295 [hep-ph/9706545].

[43] ZEUS Collaboration, Eur. Phys. J. C **55** (2008) 177 [hep-ex/0710.1498].

[44] M. Klasen, G. Kramer, Mod. Phys. Lett. A **23** (2008) 1885 [hep-ph/0806.2269].